Journal of Biomedical Optics

SPIEDigitalLibrary.org/jbo

In situ imaging of lung alveoli with an optical coherence tomography needle probe

Bryden C. Quirk
Robert A. McLaughlin
Andrea Curatolo
Rodney W. Kirk
Peter B. Noble
David D. Sampson

SPIE

In situ imaging of lung alveoli with an optical coherence tomography needle probe

Bryden C. Quirk,[a,*] Robert A. McLaughlin,[a,*] Andrea Curatolo,[a] Rodney W. Kirk,[a] Peter B. Noble,[b,c] and David D. Sampson[a,d]

[a]University of Western Australia, Optical + Biomedical Engineering Laboratory, School of Electrical, Electronic & Computer Engineering, 35 Stirling Highway, Crawley WA 6009, Australia
[b]University of Western Australia, Division of Clinical Sciences, Telethon Institute for Child Health Research, Centre for Child Health Research, 100 Roberts Road, Subiaco 6008, Australia
[c]University of Western Australia, Physiology, School of Biomedical, Biomolecular and Chemical Sciences, 35 Stirling Highway, Crawley WA 6009, Australia
[d]University of Western Australia, Centre for Microscopy, Characterisation & Analysis, 35 Stirling Highway, Crawley WA 6009, Australia

Abstract. *In situ* imaging of alveoli and the smaller airways with optical coherence tomography (OCT) has significant potential in the assessment of lung disease. We present a minimally invasive imaging technique utilizing an OCT needle probe. The side-facing needle probe comprises miniaturized focusing optics consisting of no-core and GRIN fiber encased within a 23-gauge needle. 3D-OCT volumetric data sets were acquired by rotating and retracting the probe during imaging. The probe was used to image an intact, fresh (not fixed) sheep lung filled with normal saline, and the results validated against a histological gold standard. We present the first published images of alveoli acquired with an OCT needle probe and demonstrate the potential of this technique to visualize other anatomical features such as bifurcations of the bronchioles. [DOI: 10.1117/1.3556719]

Keywords: optical coherence tomography; alveoli; lungs; pulmonary imaging; optical needle probe; interstitial.

Paper 10676LR received Dec. 23, 2010; revised manuscript received Jan. 26, 2011; accepted for publication Jan. 27, 2011; published online Mar. 22, 2011.

1 Introduction

The lungs comprise a network of branching airways, originating from the major intraparenchymal bronchi, extending to the bronchioles, and terminating in alveolar ducts that branch into alveolar sacs. The structural and mechanical properties of the alveoli regulate function: the thin walls of the alveoli are interlaced with an anastomosing network of capillaries that facilitates gas exchange; and elastin fibers within the alveoli walls allow the alveoli to expand as they fill with gas during inhalation and contract during exhalation. The lung is subject to numerous fatal pathologies that alter the structure of the alveoli and impair function.[1] Emphysema, predominantly caused by long-term exposure to cigarette smoke, is characterized by destruction of the alveoli walls and permanent enlargement of the airspaces distal to the terminal bronchioles. Pulmonary fibrosis presents as a thickening of the alveoli walls with fibrotic tissue (scar tissue). This may be secondary to other processes (e.g., asbestosis or rheumatoid arthritis), or appear without any known cause (idiopathic pulmonary fibrosis). Emphysema and pulmonary fibrosis combined account for over three quarters of all lung transplants.[2]

The assessment and development of new treatments for the above pathologies is made difficult by a lack of imaging techniques to accurately assess lung disease severity and progression. While histological analysis is the gold standard for structural assessment, it requires excision and fixation of the tissue, and so cannot be used to assess the tissue's dynamic, viscoelastic properties, which are altered in lung disease. Additionally, lung disease is inherently heterogeneous, requiring prohibitively large numbers of histological samples. This can be both time-consuming and result in procedure-related complications.

Ex vivo studies have shown that optical coherence tomography (OCT) may be used to image individual alveoli.[3,4] *In vivo* imaging of alveoli in mice[5] and rabbit models[6] has been demonstrated through use of a thoracic window, in which skin and muscle are resected from between the ribs to allow OCT imaging, and has been validated against confocal microscopy.[7] The opening can be resealed with a transparent membrane through which imaging is possible. While suitable for nonrecovery animal studies, the use of a thoracic window is undesirably invasive for human subjects.

In this paper, we propose an alternative OCT lung imaging technique that avoids the need for removal of the overlying tissue. While not a replacement for histology, this technique offers complementary information and has potential for longitudinal sampling in animal models. We utilize an OCT needle probe, where the distal focusing optics have been miniaturized and encased within a 23-gauge needle, allowing *in situ* imaging of alveoli. We present the first OCT images of alveoli acquired with an OCT needle probe and provide validation against a histological gold standard.

*These authors contributed equally to this work.

Address all correspondence to: Robert A. McLaughlin, University of Western Australia, Optical + Biomedical Engineering Laboratory, School of Electrical, Electronic & Computer Engineering, 35 Stirling Highway, Crawley WA 6009, Australia. Tel: +61 8 6488 3105; Fax: +61 8 6488 1319; E-mail: robert.mclaughlin@uwa.edu.au.

1083-3668/2011/16(3)/036009/4/$25.00 © 2011 SPIE

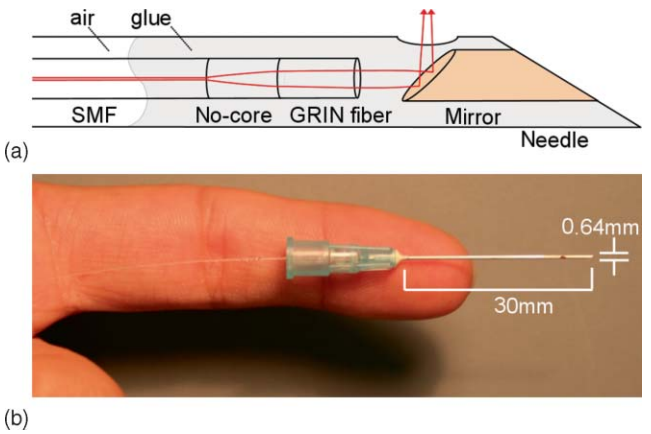

Fig. 1 (a) OCT needle probe schematic comprising single-mode fiber (SMF), no-core fiber, GRIN fiber and a mirror, (b) side-facing OCT needle probe encased in a 23-gauge needle.

2 Method

A schematic of the OCT needle probe is shown in Fig. 1. Affixed to the distal end of a length of single-mode fiber are the miniaturized focusing optics, comprising a length of no-core fiber to expand the light beam, and terminated with a length of GRIN fiber, with a pitch of 0.16, to focus the light into the tissue,[8] similar to the optical configuration described by Wu et al.[9] A small copper mirror, polished at an angle of 45 deg redirects the beam at right angles. The setup is encased in a 23-gauge needle and held rigid by embedding in optical glue (Norland, NJ, USA) within the needle. A small window is etched in the needle shaft, approximately 4 mm from the tip, through which A-scans may be acquired. The needle probe has a measured beam waist of 20 μm at a distance of 300 μm from the side window of the needle.

The probe was mounted on a stepper motor and counter-rotated at 2 Hz over a range of 6 radians to acquire 2D radial B-scans. Only clockwise rotations were used in the reconstructed 3D OCT data set, to minimize artifacts from tissue drag. A linear translation stage was used to insert and retract the needle at 7 μm per rotation. It was attached to a spectral-domain OCT system with central wavelength of 836 nm, source bandwidth of 50 nm, calculated coherence length of 6.2 μm in air, and emitting 6.8 mW of optical power onto the sample.

An intact sheep lung was obtained fresh (not fixed) and tissue usage approved by the institutional animal ethics committee. The lung was filled with normal saline until visually inflated. The OCT needle probe was inserted into several different lobes and images acquired as the needle was rotated and retracted over a distance of 2.4 mm, with a 3D scan time of approximately 3 min. The lobes were marked with ink at the location of needle insertion to aid subsequent correlation with histology. After scanning, 1×1 cm-wide sections were excised along each needle trajectory. The excised tissue was fixed, embedded in paraffin, and sectioned at 250 μm intervals in accordance with standard laboratory procedures, and haematoxylin and eosin (H&E) sections prepared. Multiplanar formatting was applied to the 3D-OCT volumetric datasets to extract the 2D image plane with an optimal match to the histological sections. The optimal match was identified by correlating multiple features over several OCT B-scans and adjacent histological slices.

3 Results

Figure 2 shows H&E histology and the matching OCT radial scan. The needle hole (labeled N) is located at the center of the images, surrounded by alveoli (labeled A in the OCT image). Each alveolar space presents as a small region of low backscatter (dark gray), incompletely delineated by the more highly backscattering alveoli walls (light gray). In the H&E image, the needle tract is identifiable as a localized defect rimmed by trauma-induced tissue artifact. Three bronchioles (labeled B1, B2, B3) can be seen adjacent to the needle hole, showing the strong geometrical correspondence between both the H&E and OCT images. Figure 2(c) highlights the value of 3-D imaging. Through the use of custom visualization software, we were able to extract arbitrary imaging planes from the volumetric OCT data. This particular view shows an image taken in a plane orthogonal to the radial B-scans, parallel to the direction of needle retraction. It shows a longitudinal view of a bronchiole,

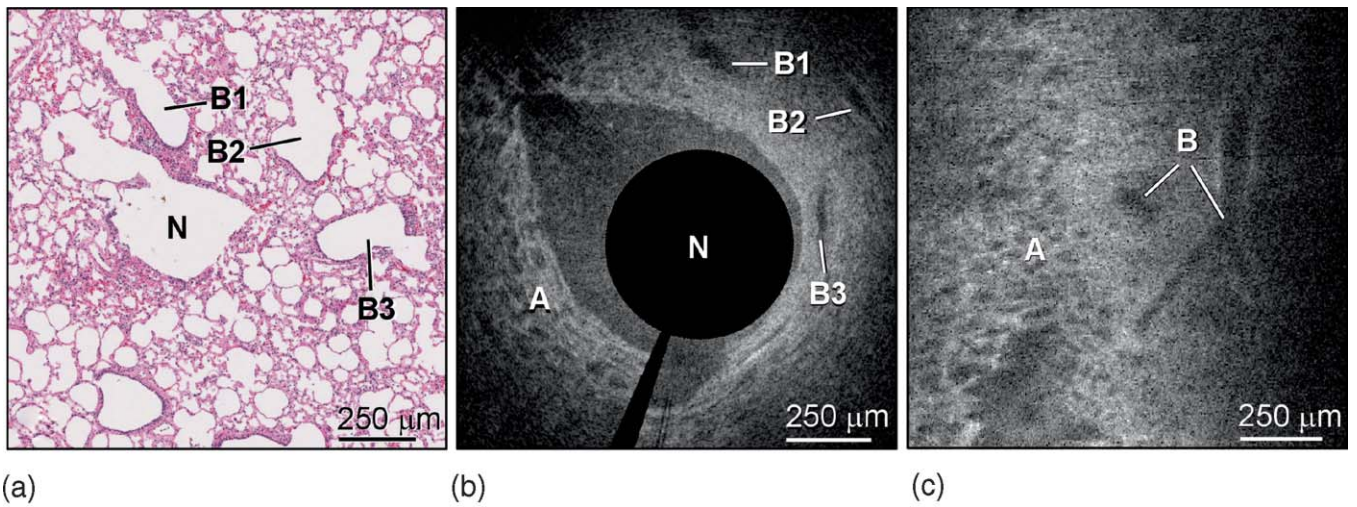

Fig. 2 (a) H&E, (b) video of radial OCT B-scan, (c) orthogonal OCT plane; N: needle hole; B: bronchiole; A: alveoli. The video in (b) shows an OCT pullback scan featuring alveoli and bronchioles (Video 1, QuickTime, 10.8 MB). [URL: http://dx.doi.org/10.1117/1.3556719.1]

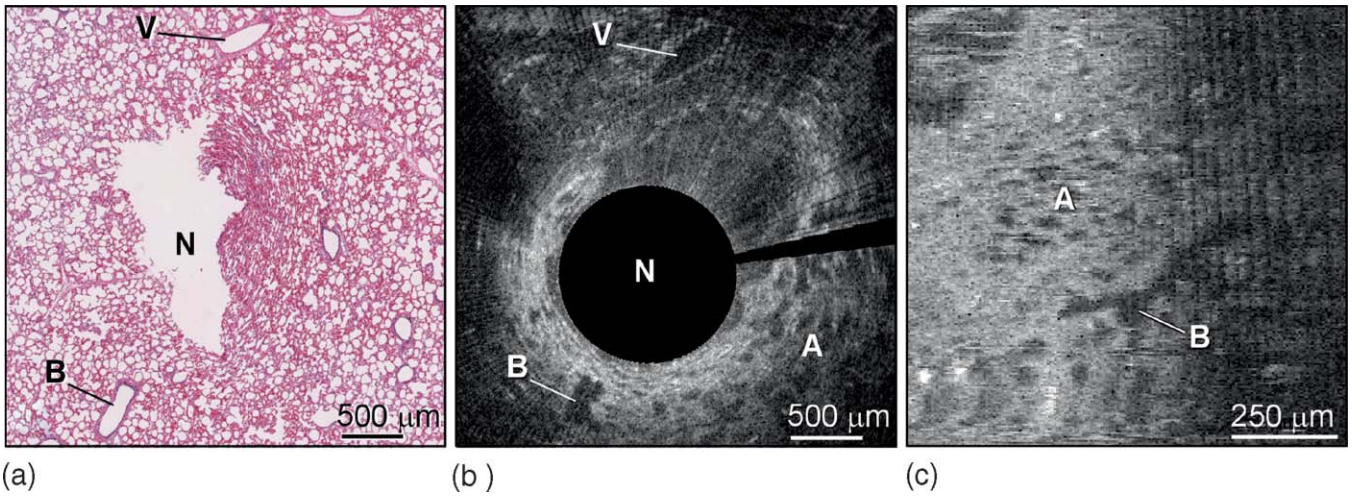

Fig. 3 (a) H&E, (b) radial OCT B-scan, (c) orthogonal OCT plane; N: needle hole; B: bronchiole; A: alveoli; V: blood vessel.

appearing as a tubular area of low backscatter (dark), bifurcating into the next generation of airways. The associated video shows the OCT pullback scan (Video 1).

Figure 3 shows H&E and OCT images of an adjacent lobe, displaying the presence of both bronchioles and a blood vessel. Some linear reconstruction artifacts appear in this OCT image due to camera settings. Adjacent radial B-scans allowed the geometry of each of the bronchioles and vessels to be tracked while within the field of view of the 3D-OCT scan, and bifurcation of the bronchiole can be seen in the orthogonal view shown in Fig. 3(c).

4 Discussion and Conclusion

The OCT images presented here show the potential of OCT to image alveoli, bronchioles, and blood vessels *in situ*. Through extraction of arbitrary imaging planes from the 3D-OCT data, we were able to visualize the shape and bifurcations of the smaller airways.

Our earlier experimental work found OCT imaging of air-filled lungs to suffer poor image penetration. This was due to the large difference in the refractive indexes of tissue and air, resulting in strong reflections at each air-tissue interface which rapidly attenuated the OCT signal. Our experiments used normal saline to reduce the refractive-index mismatch, resulting in an improved image penetration depth. Localized immersion with saline, referred to as bronchoalveolar lavage,[10] can be performed *in vivo* and is used clinically as a diagnostic test for interstitial lung disease. A bronchoscope is endoscopically positioned in the airway, and used to both flush the airway and aspirate the saline for subsequent histological analysis. More extensive flushing of the whole lung is used as treatment for pulmonary alveolar proteinosis.[11] We note that by varying the pressure of the saline and performing longitudinal imaging of a particular lung region, it may be feasible to assess the viscoelastic properties of the lung tissue, in a manner similar to that described by Williamson et al.[12] The use of a saline lavage also serves to reduce the effects of surface tension on the measured volume-pressure curve,[13] such that measurements reflect the intrinsic elastic properties of parenchymal tissue.

As with transthoracic lung biopsies, use of an external OCT needle probe carries a risk of pneumothorax. In addition, the OCT needle probe was found to cause some local trauma to pulmonary structures. While the OCT needle probe is significantly smaller than the needles currently used for lung biopsies, further reductions in its size are feasible.[14] Rotation of the OCT needle probe was also observed to cause a degree of drag on the tissue. Alternative OCT needle probe designs have been proposed to minimize this by enclosing the translating probe within a stationary catheter.[15] Anticipating the extension of this work to *in vivo* imaging, we note that movement artifact may be minimized by the temporary cessation of breathing in an anaesthetized subject.

Sampling of heterogeneous lung disease presents challenges to OCT needle imaging, as the lung may simultaneously contain both fully functional and compromised lung parenchyma. However, recent work[16] has demonstrated the potential to combine an OCT probe with a magnetic tracking system, which could allow for co-location and optimal guidance of the OCT probe to diseased areas by utilizing other imaging modalities, such as high-resolution X-ray CT. Magnetic tracking systems also allow for the potential to guide OCT needle placement to areas of localized bronchoalveolar lavage, by tracking both the saline-filled catheter and the OCT probe.

In conclusion, this paper has presented the first *in situ* images of alveoli and bronchioles acquired using an OCT needle probe, with validation against a histological gold standard. The imaging protocol utilized saline to improve OCT image penetration depth. Individual alveoli and bronchiole bifurcations were visualized. These results demonstrate the potential of needle-based OCT to provide minimally invasive *in situ* imaging of lung anatomy.

Acknowledgments

We wish to acknowledge the National Breast Cancer Foundation (Australia) for funding R.A.M. P.B.N. is supported by an NHMRC of Australia Biomedical Fellowship.

References

1. A. N. Husain and V. Kumar, "The lung," Chapter 15 in *Robbins and Cotran Pathologic Basis of Disease*, 7th ed., V. Kumar, A. K. Abbas,

and N. Fausto, Eds., pp. 711–772, Elsevier Saunders, Philadelphia (2005).
2. E. P. Trulock, L. B. Edwards, D. O. Taylor, M. M. Boucek, B. M. Keck, and M. I. Hertz, "Registry of the International Society for Heart and Lung Transplantation: Twenty-second official adult lung and heart–lung transplant report—2005," *J. Heart Lung Transplant* **24**(8), 956–967 (2005).
3. S. A. Boppart, B. E. Bouma, C. Pitris, G. J. Tearney, J. G. Fujimoto, and M. E. Brezinski, "Forward-imaging instruments for optical coherence tomography," *Opt. Lett.* **22**(21), 1618–1620 (1997).
4. N. Hanna, D. Saltzman, D. Mukai, Z. Chen, S. Sasse, J. Milliken, S. Guo, W. Jung, H. Colt, and M. Brenner, "Two-dimensional and 3-dimensional optical coherence tomographic imaging of the airway, lung, and pleura," *J. Thorac. Cardiovasc. Surg.* **129**(3), 615–622 (2005).
5. M. Mertens, A. Tabuchi, S. Meissner, A. Krueger, K. Schirrmann, U. Kertzscher, A. R. Pries, A. S. Slutsky, E. Koch, and W. M. Kuebler, "Alveolar dynamics in acute lung injury: Heterogeneous distension rather than cyclic opening and collapse," *Crit. Care Med.* **37**(9), 2604–2611 (2009).
6. S. Meissner, L. Knels, C. Schnabel, T. Koch, and E. Koch, "Three-dimensional Fourier domain optical coherence tomography *in vivo* imaging of alveolar tissue in the intact thorax using the parietal pleura as a window," *J. Biomed. Opt.* **15**(1), 016030 (2010).
7. J. Bickenbach, R. Dembinski, M. Czaplik, S. Meissner, A. Tabuchi, M. Mertens, L. Knels, W. Schroeder, P. Pelosi, E. Koch, W. M. Kuebler, R. Rossaint, and R. Kuhlen, "Comparison of two *in vivo* microscopy techniques to visualize alveolar mechanics," *J. Clin. Monit. Comput.* **23**, 323–332 (2009).
8. Y. Mao, S. Chang, S. Sherif, and C. Flueraru, "Graded-index fiber lens proposed for ultrasmall probes used in biomedical imaging," *Appl. Opt.* **46**(23), 5887–5894 (2007).
9. Y. Wu, J. Xi, L. Huo, J. Padvorac, E. J. Shin, S. A. Giday, A. M. Lennon, M. I. F. Canto, J. H. Hwang, and X. Li, "Robust high-resolution fine OCT needle for side-viewing interstitial tissue imaging," *IEEE J. Sel. Top. Quant.* **16**(4), 863–869 (2010).
10. U. Costabel, *Atlas of Bronchoalveolar Lavage*, Chapman and Hall, London (1998).
11. M. Beccaria, M. Luisetti, G. Rodi, A. Corsico, M. C. Zoia, S. Colato, P. Pochetti, A. Braschi, E. Pozzi, and I. Cerveri, "Long-term durable benefit after whole lung lavage in pulmonary alveolar proteinosis," *Eur. Respir. J.* **23**, 526–531 (2004).
12. J. P. Williamson, R. A. McLaughlin, W. J. Noffsinger, A. L. James, V. A. Baker, A. Curatolo, J. J. Armstrong, A. Regli, K. L. Shepherd, G. B. Marks, D. D. Sampson, D. R. Hillman, and P. R. Eastwood, "Elastic properties of the central airways in obstructive lung diseases measured using anatomical optical coherence tomography," *Am. J. Respir. Crit. Care Med.* **183**, 612–619 (2011).
13. J. Mead, J. L. Whittenberger, and E. P. Radford, Jr., "Surface tension as a factor in pulmonary volume-pressure hysteresis," *J. Appl. Physiol.* **10**(2), 191–196 (1957).
14. W. A. Reed, M. F. Yan, and M. J. Schnitzer, "Gradient-index fiber-optic microprobes for minimally invasive in vivo low-coherence interferometry," *Opt. Lett.* **27**(20), 1794–1796 (2002).
15. H. Li, B. A. Standish, A. Mariampillai, N. R. Munce, Y. Mao, S. Chiu, N. E. Marcon, B. C. Wilson, A. Vitkin, and V. X. D. Yang, "Feasibility of interstitial Doppler optical coherence tomography for in vivo detection of microvascular changes during photodynamic therapy," *Lasers Surg. Med.* **38**, 754–761 (2006).
16. B. Lau, R. A. McLaughlin, A. Curatolo, R. W. Kirk, D. K. Gerstmann, and D. D. Sampson, "Imaging true 3D endoscopic anatomy by incorporating magnetic tracking with optical coherence tomography: proof-of-principle for airways," *Opt. Express* **18**(26), 27173–27180 (2010).